

Reactions of the Platinum (Tri-*tert*-butylphosphine) Group with Bridging SbPh₂ Ligands in Rhenium–Antimony Carbonyl Complexes

Richard D. Adams* and William C. Pearl, Jr.

Department of Chemistry and Biochemistry, University of South Carolina, Columbia, South Carolina 29208

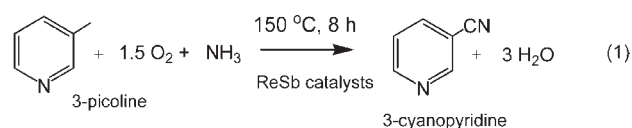
Received April 27, 2010

The reaction of [Re(CO)₄(μ-SbPh₂)₂] (1) with Pt[P(*t*-Bu)₃]₂ in *n*-octane solvent at reflux (125 °C) has yielded two platinum–rhenium–antimony compounds, Re₂(CO)₈[(μ₃-SbCH₂CMe₂)Pt(H)P(*t*-Bu)₂]P(*t*-Bu)₃(μ-SbPh₂) (2), and Re₂(CO)₈[Pt(CO)(CH₂CMe₂)P(*t*-Bu)₂](μ₃-SbPh)(μ-SbPh₂) (3), in low yields. Both products were formed by the cleavage of phenyl group(s) from one of the bridging SbPh₂ ligands in 1 and the addition of a PtP(*t*-Bu)₃ or Pt[P(*t*-Bu)₃]₂ group to the antimony atom. In both products, one of the *tert*-butyl groups was metalated on one of its methyl groups. In 2, metalation occurred on the antimony atom, while in 3, it occurred on the platinum atom. When the same reaction was performed under an atmosphere of hydrogen (1 atm), two additional new platinum–rhenium–antimony compounds, PtRe₂(CO)₈P(*t*-Bu)₃(μ₃-SbPh)(μ-SbPh₂)(μ-H) (4) and Re₂(CO)₈[PtH(CO){P(*t*-Bu)₃}] (μ₃-SbPh)(μ-SbPh₂) (5), were formed. In both products, a phenyl group was cleaved from one of the bridging SbPh₂ ligands in 1 and the addition of a PtP(*t*-Bu)₃ group to the antimony atom, but there was no metalation of the *tert*-butyl groups in these products. Instead, a hydride ligand was added to the complex. Compound 5 was also obtained from 4 by the addition of CO. Compound 4 also reacts with SbPh₃ to form the new compound PtRe₂(CO)₇P(*t*-Bu)₃(μ₃-SbPh)(μ-SbPh₂)₂ (6; 42% yield), which contains an additional bridging SbPh₂ ligand across the Pt–Re bond. The reaction of 6 with Pt[P(*t*-Bu)₃]₂ in a hydrogen atmosphere yielded the new compound Pt₂Re₂(CO)₇[P(*t*-Bu)₃]₂(μ₃-SbPh)₃ (7) by the cleavage of one phenyl ring from each of the two SbPh₂ ligands in 6 and the addition of a PtP(*t*-Bu)₃ group to the resultant SbPh ligands. Compound 7 contains three triply bridging SbPh ligands. Compounds 2–7 were each characterized by a combination of IR, NMR, and mass spectrometry spectra and single-crystal X-ray diffraction analyses.

Introduction

Antimony is known to be an important component of metal oxide catalysts used for the oxidation of hydrocarbons.¹ There are a few reports showing that rhenium–antimony oxide catalysts are also effective catalysts for the oxidation and ammoxidation of hydrocarbons.² We have recently prepared some new rhenium–antimony and rhenium–bismuth complexes that have been shown to be precursors to effective heterogeneous nanoscale catalysts for the ammoxidation of 3-picoline to 3-cyanopyridine, a precursor

to niacin, also known as vitamin B₃ under unusually mild conditions (eq 1).³



Platinum is also well-known for its ability to activate hydrocarbons,⁴ and so we have begun studies to prepare and study some rhenium–antimony–platinum complexes in the hope of preparing even better hydrocarbon oxidation catalysts.⁵

We have recently shown that the bis(phosphine) complex Pt[P(*t*-Bu)₃]₂ dissociates one of its phosphine ligands and the remaining Pt[P(*t*-Bu)₃] group can be readily added to a

*To whom correspondence should be addressed. E-mail: adams@mail.chem.sc.edu.

(1) (a) Zhang, C.; Catlow, C. R. A. *J. Catal.* **2008**, *259*, 17–25. (b) Shaikh, S.; Bethke Mamedov, E. *Top. Catal.* **2006**, *38*, 241–249. (c) Allen, M. D.; Poulston, S.; Bithell, E. G.; Goringe, M. J.; Bowker, M. *J. Catal.* **1996**, *163*, 204–214. (d) Grasselli, R. K. *Catal. Today* **1999**, *49*, 141–153. (e) Bowker, M.; Bicknell, C. R.; Kerwin, P. *Appl. Catal. A* **1996**, *136*, 205–229. (f) Nilsson, R.; Lindblad, T.; Andersson, A. *J. Catal.* **1994**, *148*, 501–513. (g) Guerrero-Perez, M. O.; Fierro, J. L. G.; Vicente, M. A.; Banares, M. A. *J. Catal.* **2002**, *206*, 399–348. (h) Guerrero-Perez, M. O.; Chang, J. S.; Hong, D. Y.; Lee, J. M.; Banares, M. A. *Catal. Lett.* **2008**, *125*, 192–196.

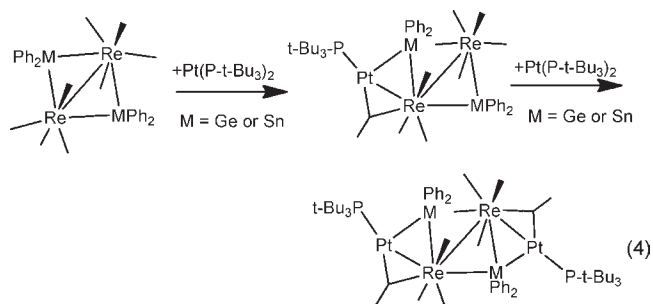
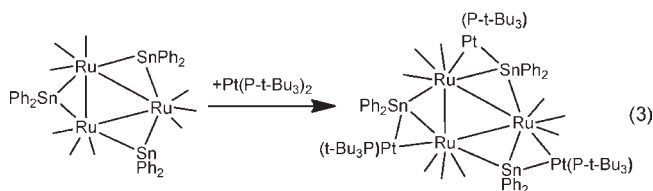
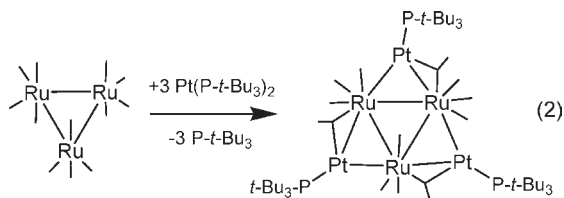
(2) (a) Liu, H.; Gaigneaux, E. M.; Imoto, H.; Shido, T.; Iwasawa, Y. *Catal. Lett.* **2008**, *71*, 75–79. (b) Liu, H.; Imoto, H.; Shido, T.; Iwasawa, Y. *J. Catal.* **2001**, *200*, 69–78. (c) Gaigneaux, E. M.; Liu, H.; Imoto, H.; Shido, T.; Iwasawa, Y. *Top. Catal.* **2000**, *11/12*, 185–193.

(3) Raja, R.; Adams, R. D.; Blom, D. A.; Pearl, W. C., Jr.; Gianotti, E.; Thomas, J. M. *Langmuir* **2009**, *25*, 7200–7204.

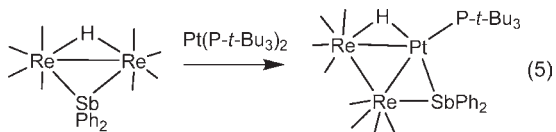
(4) (a) Burch, R.; Garla, L. C. *J. Catal.* **1981**, *71*, 360–372. (b) Somorjai, G.; Blakely, D. W. *Nature* **1975**, *258*, 580–583. (c) Burch, R.; Hayes, M. J. *J. Mol. Catal. A: Chem.* **1995**, *100*, 13–33. (d) Zhong, H. A.; Labinger, J. A.; Bercaw, J. E. *J. Am. Chem. Soc.* **2002**, *124*, 1378–1399. (e) Fekl, U.; Goldberg, K. I. *Adv. Inorg. Chem.* **2003**, *54*, 259–320.

(5) Adams, R. D.; Hall, M. B.; Pearl, W. C., Jr.; Yang, X. *Inorg. Chem.* **2009**, *48*, 652–662.

variety of metal–metal bonds in polynuclear metal carbonyl complexes, e.g., eqs 2–4.^{6–10}



We have also investigated the reaction of the antimony-bridged dirhenium carbonyl complex $\text{Re}(\text{CO})_8(\mu\text{-SbPh}_2)(\mu\text{-H})$ ¹¹ with $\text{Pt}[\text{P}(t\text{-Bu})_3]_2$.⁵ The major product obtained from this reaction was formed by the addition of a $\text{Pt}[\text{P}(t\text{-Bu})_3]$ group to the dirhenium complex with insertion of the platinum atom into one of the $\text{Re}\text{--}\text{Sb}$ bonds (eq 5).



We have recently synthesized the doubly bridged antimony compound $[\text{Re}(\text{CO})_4(\mu\text{-SbPh}_2)]_2$ (**1**) from a thermal transformation of the compound $\text{ReH}(\text{CO})_4(\text{SbPh}_3)$.³ For the purposes of comparison with the reactions of compounds $[\text{Re}(\text{CO})_4(\mu\text{-SnPh}_2)]_2$ and $\text{Re}_2(\text{CO})_8(\mu\text{-SbPh}_2)(\mu\text{-H})$, we have now investigated the reaction of **1** with $\text{Pt}[\text{P}(t\text{-Bu})_3]_2$ in both the presence and absence of H_2 . Several new ReSbPt compounds have been isolated that reveal a pattern of reactivity

around the $\text{Sb}\text{--}\text{Ph}$ bonds that is accompanied by activation of the $\text{C}\text{--}\text{H}$ bonds on the methyl groups of the *tert*-butyl groups of the $\text{P}(t\text{-Bu})_3$ ligands on the platinum atom and cluster growth processes involving triply bridging SbPh ligands. These results are reported herein.

Experimental Section

General Data. Reagent-grade solvents were dried by the standard procedures and were freshly distilled prior to use. IR spectra were recorded on a Thermo Nicolet Avatar 360 FT-IR spectrophotometer. ^1H NMR and $^{31}\text{P}\{^1\text{H}\}$ NMR were recorded on a Varian Mercury 400 spectrometer operating at 400.1 and 161.9 MHz, respectively. $^{31}\text{P}\{^1\text{H}\}$ NMR spectra were externally referenced against 85% *o*- H_3PO_4 . Mass spectrometric (MS) measurements performed by a direct-exposure probe using electron impact ionization (EI) were made on a VG 70S instrument. $\text{Pt}[\text{P}(t\text{-Bu})_3]_2$, SbPh_3 , and $\text{Re}_2(\text{CO})_{10}$ were obtained from Strem and were used without further purification. $\text{Re}_2(\text{CO})_8(\mu\text{-SbPh}_2)_2$ (**1**) was prepared as previously reported.³ Product separations were performed by thin-layer chromatography (TLC) in air on Analtech 0.25 and 0.5 mm silica gel 60 Å F_{254} glass plates.

Reaction of $\text{Pt}[\text{P}(t\text{-Bu})_3]_2$ with **1 at 125 °C.** A total of 35.5 mg (0.0592 mmol) of $\text{Pt}[\text{P}(t\text{-Bu})_3]_2$ was added to a solution of 19.9 mg (0.0173 mmol) of **1** dissolved in 20 mL of octane and was refluxed for 3 h. After cooling, the solvent was removed in vacuo. The products were then isolated by TLC by using a 3:1 hexane/methylene chloride solvent mixture. This yielded, in order of elution, 12.0 mg of colorless unreacted **1**, a yellow band of $\text{Re}_2(\text{CO})_8(\mu\text{-SbCH}_2\text{CMe}_2)\text{Pt}(\text{H})\text{P}(t\text{-Bu})_2\text{P}(t\text{-Bu})_3(\mu\text{-SbPh}_2)$ (**2**; 2.2 mg, 9% yield), and a colorless band of $\text{Re}_2(\text{CO})_8[\text{Pt}(\text{CH}_2\text{CMe}_2)\text{P}(t\text{-Bu})_2](\mu_3\text{-SbPh})(\mu\text{-SbPh}_2)$ (**3**; 3.3 mg, 13% yield). Spectral data for **2**: IR [ν_{CO} (cm^{-1}) in a hexane solvent] 2067(w), 2046(s), 1995(w), 1990(w), 1978(m), 1968(vs), 1953(vw) 1938(s); ^1H NMR (400 MHz, TCE, 25 °C, TMS) δ 7.3–7.8 (m, Ph, 10H), 3.6 (d, $-\text{CH}_2$, 1H, $^2J_{\text{H-H}} = 13$ Hz), 2.8 (d, $-\text{CH}_2$, 1H, $^2J_{\text{H-H}} = 13$ Hz, $^3J_{\text{P-H}} = 40$ Hz, $^3J_{\text{Pt-H}} = 22$ Hz), 1.9 (d, $-\text{CH}_3$, 6H, $^2J_{\text{P-H}} = 7$ Hz), 1.6 (d, *t*-Bu, 27H, $^2J_{\text{P-H}} = 12$ Hz), 1.4 (d, Bu^t, 18H, $^2J_{\text{P-H}} = 12$ Hz), 1.4 (d, $-\text{CH}_3$, 3H, $^2J_{\text{P-H}} = 12$ Hz), -11.8 (d, hydride, 1H, $^2J_{\text{P-H}} = 22$ Hz, $^1J_{\text{Pt-H}} = 979$ Hz); ^{31}P NMR δ 128.1 (d, P, $^1J_{\text{Pt-P}} = 2638$ Hz), 96.9 (d, P, $^1J_{\text{Pt-P}} = 2806$ Hz); EI/MS m/z 1594 (M^+), 1566 ($\text{M}^+ - \text{CO}$), 1538 ($\text{M}^+ - 2\text{CO}$). The isotope pattern is consistent with the presence of two rhenium, one platinum, and two antimony atoms. Spectral data for **3**: IR [ν_{CO} (cm^{-1}) in a hexane solvent] 2074(vw), 2055(m), 2044(w), 2009(vw), 1987(s), 1976(vs), 1963(vw), 1944(s); ^1H NMR (400 MHz, TCE, 25 °C, TMS) δ 7.2–7.6 (m, Ph, 15H), 1.4 (d, *t*-Bu, 18H, $^2J_{\text{P-H}} = 14$ Hz), 1.4 (d, $-\text{CH}_3$, 6H, $^3J_{\text{P-H}} = 16$ Hz), 1.2 (d, $-\text{CH}_2$, 2H, $^3J_{\text{P-H}} = 13$ Hz); ^{31}P NMR δ -3.5 (d, $^1J_{\text{Pt-P}} = 1641$ Hz); EI/MS m/z 1496 (M^+), 1468 ($\text{M}^+ - \text{CO}$), 1440 ($\text{M}^+ - 2\text{CO}$), 1412 ($\text{M}^+ - 3\text{CO}$), 1384 ($\text{M}^+ - 4\text{CO}$). The isotope pattern is consistent with the presence of two rhenium, one platinum, and two antimony atoms.

Reaction of $\text{Pt}[\text{P}(t\text{-Bu})_3]_2$ **1 at 125 °C under a Hydrogen Atmosphere.** A total of 15.3 mg (0.0255 mmol) of $\text{Pt}[\text{P}(t\text{-Bu})_3]_2$ was added to a solution of 8.7 mg (0.00758 mmol) of **1** dissolved in 10 mL of octane and was refluxed while purging with hydrogen gas for 2 h. The solvent was removed in vacuo, and the product was then isolated by TLC by using a 4:1 hexane/methylene chloride solvent mixture to yield, in order of elution, a colorless band of **1** (0.7 mg, 8% yield), a colorless band of $\text{PtRe}_2(\text{CO})_8\text{P}(t\text{-Bu})_3(\mu_3\text{-SbPh})(\mu\text{-SbPh}_2)(\mu\text{-H})$ (**5**; 0.5 mg, 4% yield), and a yellow band of $\text{Re}_2(\text{CO})_8[\text{PtH}(\text{CO})\{\text{P}(t\text{-Bu})_3\}](\mu_3\text{-SbPh})(\mu\text{-SbPh}_2)$ (**4**; 2.9 mg, 26% yield). Spectral data for **4**: IR [ν_{CO} (cm^{-1}) in a hexane solvent] 2072(m), 2048(w), 2009(vs), 1990(s), 1971(s), 1953(s), 1928(m), 1916(m); ^1H NMR (400 MHz, CDCl_3 , 25 °C, TMS) δ 7.0–7.6 (m, Ph, 15H), 1.4 (d, *t*-Bu, 27H, $^2J_{\text{P-H}} = 14$ Hz), -6.8 (d, hydride, 1H, $^1J_{\text{Pt-H}} = 623$ Hz, $^2J_{\text{P-H}} = 14$ Hz); ^{31}P NMR δ 78.0 (s, P, $^1J_{\text{Pt-P}} = 2717$ Hz); EI/MS m/z 1470 (M^+), 1442 ($\text{M}^+ - 2\text{CO}$), 1336 ($\text{M}^+ - 2\text{CO} - \text{C}_6\text{H}_6$). The isotope pattern is consistent with the presence of two rhenium, one platinum, and two antimony atoms.

(6) (a) Adams, R. D.; Captain, B. *Acc. Chem. Res.* **2009**, *42*, 409–418. (b) Adams, R. D.; Boswell, E. M.; Captain, B.; Zhu, L. *J. Cluster Sci.* **2008**, *19*, 121–132.

(7) Adams, R. D.; Captain, B.; Hall, M. B.; Trufan, E.; Yang, X. *J. Am. Chem. Soc.* **2007**, *129*, 12328–12340.

(8) Adams, R. D.; Trufan, E. *Organometallics* **2008**, *27*, 4108–4115.

(9) Adams, R. D.; Captain, B.; Trufan, E. *J. Organomet. Chem.* **2008**, *693*, 3593–3602.

(10) Adams, R. D.; Captain, B.; Herber, R. H.; Johansson, M.; Nowik, I.; Smith, J. L., Jr.; Smith, M. D. *Inorg. Chem.* **2005**, *44*, 6346–6358.

(11) Adams, R. D.; Captain, B.; Pearl, W. C., Jr. *J. Organomet. Chem.* **2008**, *693*, 1636–1644.

Spectral data for **5**: IR [ν_{CO} (cm^{-1}) in a hexane solvent] 2075(vw), 2057(s), 2031(w), 1988(vs), 1979(vs), 1965(w), 1946-(vs); ^1H NMR (400 MHz, CDCl_3 , 25 °C, TMS) δ 6.9–7.6 (m, Ph, 15H), 1.4 (d, *t*-Bu, 27H, $^2J_{\text{P-H}} = 13$ Hz), –3.8 (d, hydride, 1H, $^1J_{\text{Pt-H}} = 781$ Hz, $^2J_{\text{P-H}} = 14$ Hz); ^{31}P NMR δ 89.1 (s, P, $^1J_{\text{Pt-P}} = 2417$ Hz); EI/MS m/z 1498 (M^+), 1470 ($\text{M}^+ - \text{CO}$), 1442 ($\text{M}^+ - 2\text{CO}$), 1336 ($\text{M}^+ - 2\text{CO} - \text{C}_6\text{H}_6$). The isotope pattern is consistent with the presence of two rhenium, one platinum, and two antimony atoms.

Addition of CO to 4. A total of 2.1 mg of **4** was dissolved in 5 mL of methylene chloride and purged with carbon monoxide for 2 h at 25 °C. The solvent was removed in vacuo, and the product **5** was then isolated by TLC by using a 4:1 hexane/methylene chloride solvent mixture to yield 0.6 mg of **5** (28% yield) and 1.5 mg of **4** recovered (71%).

Addition of SbPh₃ to 4. A total of 5.7 mg (0.0162 mmol) of SbPh₃ was added to a solution of 7.6 mg (0.00517 mmol) of **4** dissolved in 10 mL of octane, and the solution was refluxed for 2.5 h. After cooling, the solvent was removed in vacuo. The product was then isolated by TLC by using a 4:1 hexane/methylene chloride solvent mixture to yield an orange band of $\text{PtRe}_2(\text{CO})_7\text{P}(\text{t-Bu})_3(\mu_3\text{-SbPh})_2$ (**6**; 3.7 mg, 42%). Spectral data for **6**: IR [ν_{CO} (cm^{-1}) in a hexane solvent] 2073(m), 2007(vs), 1989(w), 1981(m), 1951(s), 1929(w); ^1H NMR (400 MHz, CD_2Cl_2 , 25 °C, TMS) δ 6.6–7.8 (m, Ph, 25H), 1.6 (d, *t*-Bu, 27H, $^2J_{\text{P-H}} = 13$ Hz), 132.2 (s, P, $^1J_{\text{Pt-P}} = 5323$ Hz); EI/MS m/z 1716 (M^+), 1659 ($\text{M}^+ - 2\text{CO}$); UV–vis (in a CH_2Cl_2 solvent) λ_{max} 418 nm ($\epsilon = 1.016 \times 10^4 \text{ mol}^{-1} \text{ cm}^{-1}$), 485 ($3.559 \times 10^3 \text{ mol}^{-1} \text{ cm}^{-1}$). The isotope pattern is consistent with the presence of two rhenium, one platinum, and three antimony atoms.

Addition of Pt[P(*t*-Bu)₃]₂ to 6. A total of 15.8 mg (0.0234 mmol) of Pt[P(*t*-Bu)₃]₂ was added to a solution of 16.0 mg (0.00933 mmol) of **6** dissolved in 20 mL of octane. The solution was refluxed under a strong purge of hydrogen for 4 h. The solvent was then removed in vacuo, and the products were isolated by TLC by using a 4:1 hexane/methylene chloride solvent mixture to yield 6.3 mg of unreacted **6**. A brown band of that gave 2.2 mg of $\text{Pt}_2\text{Re}_2(\text{CO})_7[\text{P}(\text{t-Bu})_3]_2(\mu_3\text{-SbPh})_3$ (**7**; 12% yield). Spectral data for **7**: IR [ν_{CO} (cm^{-1}) in a hexane solvent] 2067(m), 1994-(vs), 1973(s), 1946(s), 1931(m); ^1H NMR (400 MHz, CD_2Cl_2 , 25 °C, TMS) δ 7.0–8.1 (m, Ph, 15H), 1.4 (d, *t*-Bu, 54H, $^2J_{\text{P-H}} = 13$ Hz); ^{31}P NMR δ 125.3 (s, P, $^1J_{\text{Pt-P}} = 5254$ Hz); EI/MS m/z 1960 (M^+), 1960 ($\text{M}^+ - 2\text{CO}$). UV–vis (in a CH_2Cl_2 solvent) $\lambda_{\text{max}} = 736$ nm ($\epsilon = 1.018 \times 10^3 \text{ mol}^{-1} \text{ cm}^{-1}$). The isotope pattern is consistent with the presence of two rhenium, two platinum, and three antimony atoms.

Addition of Pt[P(*t*-Bu)₃]₂ to 6 in a Sealed NMR Tube. A total of 6.0 mg (0.0100 mmol) of Pt[P(*t*-Bu)₃]₂ was added to a solution of 15.3 mg (0.00892 mmol) of **6** dissolved in toluene-*d*⁸ in an NMR tube. The tube was filled with hydrogen and heated at 108 °C for 1.5 h. An ^1H NMR spectrum was then recorded, which showed the formation of C_6H_6 . The solvent was removed in vacuo, and the product was then isolated by TLC by using a 3:1 hexane/methylene chloride solvent mixture to yield an orange band of unreacted **6** (6.8 mg) and a small amount of brown **7** (0.7 mg, 4%).

Alternative Synthesis of 6 and 7. A total of 23.0 mg (0.0384 mmol) of Pt[P(*t*-Bu)₃]₂ was added to a solution of 24.3 mg (0.165 mmol) of $\text{Re}_2(\mu\text{-SbPh})_2\text{SbPh}_3(\text{CO})_7$ (**8**)¹¹ dissolved in 20 mL of octane, and the resulting solution was refluxed with hydrogen purging for 2 h. The solvent was removed in vacuo, and the product was then isolated by TLC by using a 4:1 hexane/methylene chloride solvent mixture to yield a colorless band of unreacted **8** (11.3 mg, 47% yield), an orange band of **6** (5.3 mg, 19% yield), and a brown band of **7** (3.3 mg, 10% yield).

Crystallographic Analyses. Single crystals of **2** and yellow **3** suitable for X-ray diffraction were obtained by the slow evaporation of solvent from solutions in a benzene/octane solvent mixture at 5 °C. Single crystals of yellow **4** and **5**, orange **6**, and brown **7** suitable for X-ray diffraction were obtained by the slow

evaporation of solvent from solutions in a methylene chloride/hexane solvent mixture at –25 °C. Each data crystal was glued onto the end of a thin glass fiber. X-ray intensity data were measured by using a Bruker SMART APEX CCD-based diffractometer by using Mo K α radiation ($\lambda = 0.71073$ Å). The raw data frames were integrated with the S AINT^+ program by using a narrow-frame integration algorithm.¹² Correction for Lorentz and polarization effects was also applied with S AINT^+ . An empirical absorption correction based on the multiple measurement of equivalent reflections was applied using the S ADABS program. All structures were solved by a combination of direct methods and difference Fourier syntheses and refined by full-matrix least squares on F^2 , using the S HELXTL software package.¹³ All non-hydrogen atoms were refined with anisotropic thermal parameters. Unless indicated otherwise, the hydrogen atoms were placed in geometrically idealized positions and included as standard riding atoms during the least-squares refinements. Crystal data, data collection parameters, and results of the refinements are listed in Table 1. Compounds **4**, **5**, and **7** all crystallized in the triclinic crystal system. The space group $P\bar{1}$ was assumed for each and was confirmed by the successful solution and refinement of the structure. For each of these analyses, there is one complete independent molecule of the complex in the asymmetric crystal unit. In the analysis of **4**, the hydrido ligand was located in the difference Fourier map along the Re–Pt bond. It was refined by using the constraint M–H equal to 1.75 Å. The hydrido ligand in **5** was located and refined on its three positional parameters with an isotropic thermal parameter. Compound **6** crystallized in the orthorhombic crystal system. The space group $P2_12_12_1$ was confirmed for **6** on the basis of the systematic absences observed in the data. Compound **6** contains one independent molecule present in the asymmetric crystal unit. Compounds **2** and **3** crystallized in the monoclinic crystal system. The space group $P2_1/n$ was confirmed for **2** on the basis of the systematic absences observed in the data. The space group $P2_1/c$ was selected for **3** on the basis of the systematic absences observed in the data. The hydrido ligand in **2** was located and refined on its positional parameters with an isotropic thermal parameter. The structure of **2** contained two disordered orientations for the phosphine ligand and the antimony atom. The *t*-Bu groups were refined by setting the C–C distance equal to 1.55 Å for C41–C44 and using the same command to restrain the C–C distances of the remaining *t*-Bu groups to the same value. The weighting scheme for the two disordered orientations was then refined and converged to final values of 71 and 29. The structure of **7** contained two disordered orientations for the PtP(*t*-Bu)₃ and phenyl groups. The *t*-Bu groups were refined by setting the C–C bond distance equal to 1.55 Å in C43–C46 and then using the same command to constrain the C–C bond distances in the remaining *t*-Bu groups. The weighting scheme for the two disordered orientations was then refined and converged to final values of 56 and 44. The disordered phenyl group C26–C30 was refined with two orientations to final values of 77 and 23.

Results

Two compounds, **2** (9% yield) and **3** (13% yield), were obtained in low yields from the reaction of **1** with Pt[P(*t*-Bu)₃]₂ in a solution in *n*-octane solvent at reflux (125 °C) over a 3 h period. Both compounds were characterized by a combination of IR, NMR, and MS spectrometry and single-crystal X-ray diffraction analyses. An ORTEP diagram of the molecular structure of **2** is shown in Figure 1. The structure of **2** consists of a Re_2Sb_2 rhombus with a cyclometalated Pt(CH_2CMe_2)P(*t*-Bu)₂ group attached to one of the antimony atoms, Sb2. Both phenyl rings have been cleaved from that

(12) S AINT^+ , version 6.2a; Bruker Analytical X-ray System, Inc.: Madison, WI, 2001.

(13) Sheldrick, G. M. S HELXTL , version 6.1; Bruker Analytical X-ray Systems, Inc.: Madison, WI, 1997.

Table 1. Crystallographic Data for the Structural Analyses of Compounds 2–7

	2	3	4
empirical formula	Re ₂ Sb ₂ PtP ₂ -O ₈ C ₄₄ H ₆₃	Re ₂ Sb ₂ PtP-O ₉ C ₃₉ H ₄₁	Re ₂ Sb ₂ Pt-PO ₈ C ₃₈ H ₄₃
fw	1592.87	1495.68	1469.68
cryst syst	monoclinic	monoclinic	triclinic
lattice parameters			
<i>a</i> (Å)	9.7180(5)	9.2736(3)	11.9389(10)
<i>b</i> (Å)	36.1259(19)	20.8500(8)	12.3349(10)
<i>c</i> (Å)	15.0511(8)	23.7667(9)	17.6383(14)
α (deg)	90	90	109.279(1)
β (deg)	98.443(1)	94.200(1)	90.146(2)
γ (deg)	90	90	115.790(1)
<i>V</i> (Å ³)	5226.7(5)	4583.1(3)	2174.7(3)
space group	<i>P</i> 2 ₁ / <i>n</i>	<i>P</i> 2 ₁ / <i>c</i>	<i>P</i> $\bar{1}$
<i>Z</i> value	4	2	2
ρ_{calc} (g/cm ³)	2.024	2.168	2.244
μ (Mo K α) (mm ⁻¹)	8.408	9.550	10.059
temperature (K)	294(2)	294(2)	294(2)
2 θ_{max} (deg)	52.74	52.74	56.7
no. of obsd reflns [<i>I</i> > 2 σ (<i>I</i>)]	7588	5834	7581
no. of param	638	480	482
GOF	1.081	1.016	1.011
max shift in the cycle	0.002	0.002	0.001
residuals ^a : R1; wR2	0.0476; 0.0990	0.0481; 0.1109	0.0486; 0.1064
abs coeff: max/min	1.000/0.535	1.000/0.525	1.000/0.558
largest peak in final diff. map (e/Å ³)	2.028	1.913	2.582

	5	6	7
empirical formula	Re ₂ Sb ₂ Pt-PO ₉ C ₃₉ H ₄₃	Re ₂ Sb ₃ Pt-PO ₇ C ₄₉ H ₅₂	Re ₂ Sb ₃ Pt ₂ -P ₂ O ₇ C ₄₉ H ₆₉
fw	1497.69	1716.62	1959.81
cryst syst	triclinic	orthorhombic	triclinic
lattice parameters			
<i>a</i> (Å)	9.2812(17)	13.2975(16)	12.3000(10)
<i>b</i> (Å)	13.585(3)	16.2231(16)	13.9922(11)
<i>c</i> (Å)	19.413(4)	24.402(3)	18.8826(14)
α (deg)	96.997(4)	90	104.339(2)
β (deg)	92.866(4)	90	94.029(2)
γ (deg)	105.465(4)	90	111.518(2)
<i>V</i> (Å ³)	2332.8(7)	5264.2(11)	2881.9(4)
space group	<i>P</i> $\bar{1}$	<i>P</i> 2 ₁ 2 ₁	<i>P</i> $\bar{1}$
<i>Z</i> value	2	4	2
ρ_{calc} (g/cm ³)	2.132	2.166	2.258
μ (Mo K α) (mm ⁻¹)	9.381	8.821	10.501
temperature (K)	294(2)	294(2)	294(2)
2 θ_{max} (deg)	52.74	56.54	52.74
no. of obsd reflns [<i>I</i> > 2 σ (<i>I</i>)]	5880	10589	7148
no. of param	499	577	604
GOF	0.997	1.024	1.002
max shift in the cycle	0.000	0.001	0.001
residuals ^a : R1; wR2	0.0672; 0.1484	0.0349; 0.0635	0.0630; 0.1086
abs coeff: max/min	1.000/0.568	1.000/0.564	1.000/0.572
largest peak in final diff. map (e/Å ³)	2.884	1.504	1.982

$$^a R1 = \frac{\sum_{hkl} (|F_{\text{obs}}| - |F_{\text{calc}}|)}{\sum_{hkl} |F_{\text{obs}}|}; wR2 = \frac{[\sum_{hkl} w(|F_{\text{obs}}| - |F_{\text{calc}}|)^2]}{[\sum_{hkl} w F_{\text{obs}}^2]}^{1/2}, w = 1/\sigma^2(F_{\text{obs}}); GOF = \frac{[\sum_{hkl} w (|F_{\text{obs}}| - |F_{\text{calc}}|)^2]}{(n_{\text{data}} - n_{\text{vari}})^{1/2}}.$$

antimony atom. This antimony atom is coordinated to the platinum atom, Pt1–Sb2 = 2.7166(10) Å; both rhenium atoms and the carbon atom C40 of a methylene group formed by the cleavage of a hydrogen atom from one of the methyl groups of one of the *t*-butyl groups from one of the P(*t*-Bu)₃ ligands on the Pt[P(*t*-Bu)₃]₂ reagent. The Sb–C distance, Sb2–C40 = 2.193(14) Å, to the metalated CH₂ group is slightly longer than the Sb–C distances to the phenyl rings of the bridging SbPh₂ group, Sb1–C25 = 2.139(10) Å and Sb1–C31 = 2.140(11) Å. The Re–Sb distances to Sb2, Re1–Sb2 = 2.8831(9) Å and

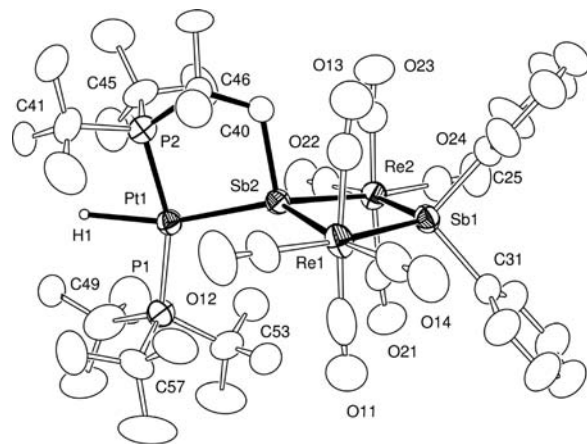


Figure 1. ORTEP diagram of the molecular structure of **2** showing 40% probability thermal ellipsoids. The hydrogen atoms on the ligands are omitted for clarity. Selected bond distances (Å) and angles (deg) are as follows: Pt1–Sb2 2.7166(10), Pt1–H1 2.07(17), Re1–Sb1 2.7210(7), Re1–Sb2 2.8831(9), Re2–Sb1 2.7204(7), Re2–Sb2 2.9083(10), Sb1–C25 2.139(10), Sb1–C31 2.140(11), Sb2–C40 2.193(14); C40–Sb2–Pt1 92.1(4).

Re2–Sb2 = 2.9083(10) Å, are much longer than the Re–Sb distances to the bridging SbPh₂ group, Re1–Sb1 = 2.7210(7) Å and Re2–Sb1 = 2.7204(7) Å. This lengthening may be due to steric interactions between the CO ligands on the rhenium atoms and the P(*t*-Bu)₃ ligand on the platinum atom. There is a hydrido ligand located on the platinum atom, Pt1–H1 = 2.07(17) Å, trans to the Pt–Sb bond. The position of the hydrido ligand was further confirmed by its high-field ¹H NMR shift, δ –11.8 (d, ²*J*_{P–H} = 22 Hz), and its large one-bond coupling to the platinum atom, ¹*J*_{Pt–H}¹⁹⁵ = 979 Hz. The five-membered cyclometalated ring is conformationally rigid on the ¹H NMR time scale at room temperature because separate resonances were observed for the inequivalent methylene protons on C40 [δ 3.6 (d, –CH₂, 1H, ²*J*_{H–H} = 13 Hz), 2.8 (d, –CH₂, 1H, ²*J*_{H–H} = 13 Hz, ³*J*_{P–H} = 40 Hz, ³*J*_{Pt–H} = 22 Hz)] and the two inequivalent methyl groups on C37 [δ 1.9 (d, –CH₃, 3H, ²*J*_{P–H} = 7 Hz), 1.4 (d, –CH₃, 3H, ²*J*_{P–H} = 12 Hz)]. However, at temperatures only slightly above room temperature, these resonances broadened and coalesced reversibly, indicating the onset of inversion of the configuration of the puckered five-membered ring. Formally, both rhenium atoms in **2** are in the 1+ oxidation state and have 18-electron configurations; the platinum atom is in the 2+ oxidation state and has a 16-electron configuration. There is no Re–Re bond present in **2**, Re1···Re2 = 4.373(1) Å.

An ORTEP diagram of the molecular structure of **3** is shown in Figure 2. As in **2**, the structure of **3** consists of a Re₂Sb₂ rhombus with a cyclometalated Pt(CH₂CMe₂)P(*t*-Bu)₂ group, but the ring contains only four atoms because the methylene group C50 is bonded to the platinum atom instead of the antimony atom, Pt1–C50 = 2.08(3) Å. Metalation of the methyl groups on *t*-Bu groups of the phosphine ligands coordinated to platinum atoms has been observed on numerous previous occasions.¹⁴ The antimony atom Sb2 is coordinated to the

(14) (a) Adams, R. D.; Captain, B.; Fu, W.; Smith, M. D.; Zhu, L. *Inorg. Chem.* **2006**, *45*, 430–436. (b) Adams, R. D.; Captain, B.; Zhu, L. *J. Organomet. Chem.* **2008**, *693*, 819–833. (c) Goel, A. B.; Goel, S.; Van Derveer, D. *Inorg. Chim. Acta* **1981**, *54*, L267. (d) Goel, A. B.; Goel, S.; Van Derveer, D. *Inorg. Chim. Acta* **1984**, *82*, L9. (e) Mullica, D. F.; Sappenfield, E. L.; Leschnitzer, D. H. *Acta Crystallogr., Sect. C* **1991**, *47*, 874. (f) Goel, A. B.; Goel, S.; Van Derveer, D.; Clark, H. C. *Inorg. Chim. Acta* **1981**, *53*, 117.

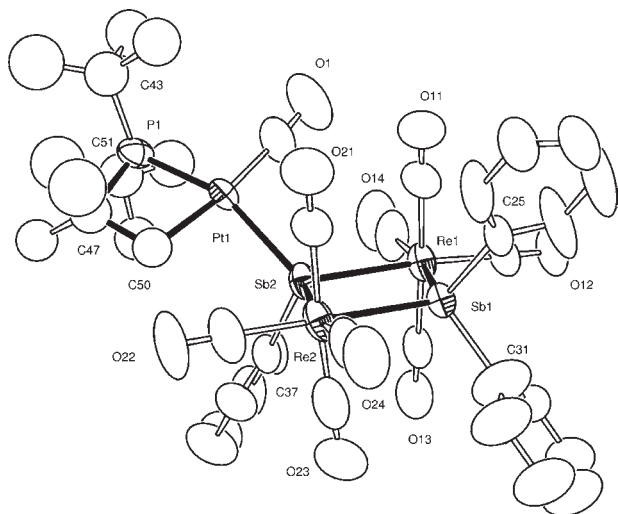


Figure 2. ORTEP diagram of the molecular structure of **3** showing 30% probability thermal ellipsoids. The hydrogen atoms on the ligands are omitted for clarity. Selected interatomic bond distances (Å) and angles (deg) are as follows: Pt1–Sb2 2.671(5), Pt1–C50 2.08(3), Re1–Sb1 2.7432(8), Re1–Sb2 2.7946(8), Re2–Sb1 2.7379(8), Re2–Sb2 2.7905(9); C50–Pt1–P1 70.6(7).

platinum atom, Pt1–Sb2 = 2.671(5) Å, but unlike **2**, one of its two original phenyl groups is still bonded to it. The Re–Sb bond distances, Re1–Sb2 = 2.7946(8) Å and Re2–Sb2 = 2.7905(9) Å, are considerably shorter than those involving the cyclometalated ring in compound **2**. There are four linear terminal carbonyl ligands on each rhenium atom and one on the platinum atom. Formally, each of the rhenium atoms in **3** has a 1+ oxidation state and an 18-electron configuration. The platinum atom has a 2+ oxidation state and a 16-electron configuration. There is no Re–Re bond present in **3**, Re1···Re2 = 4.342(1) Å. The hydrogen atom from the metalated methyl group was probably combined with the missing phenyl group from the antimony atom Sb2 and eliminated from the complex as benzene.

When compound **1** was allowed to react with Pt[P(*t*-Bu)₃]₂ in a solution in *n*-octane solvent at reflux under an atmosphere of hydrogen, two compounds, **4** and **5**, were obtained in 26% and 4% yield, respectively. Compounds **4** and **5** were also characterized by a combination of IR, NMR, and MS spectra and single-crystal X-ray diffraction analyses. An ORTEP diagram of the molecular structure of **4** is shown in Figure 3. As with **2** and **3**, the structure of **4** also consists of a Re₂Sb₂ rhombus. One of the phenyl rings on atom Sb2 was eliminated from the reagent **1**, and a PtP(*t*-Bu)₃ group and one hydrido ligand were added to the complex. The PtP(*t*-Bu)₃ group bridges the Re1–Sb2 bond, Pt1–Sb2 = 2.6493(7) Å and Pt1–Re1 = 3.0235(5) Å, and one of the CO ligands from Re1 was shifted to the platinum atom. The Re1–Sb2 bond distance is shorter than all of the other Re–Sb bonds, 2.6839(7) Å, probably because of the presence of the bridging platinum atom. There is a hydrido ligand bridging the Re1–Pt1 bond, which helps to explain the long length of this bond.¹⁵ The hydrido exhibits the expected high-field NMR shift, δ –3.8, with strong coupling to platinum, ¹J_{Pt–H} = 781 Hz and ²J_{P–H} = 14 Hz. Formally, both rhenium atoms are in the 1+ oxidation state in **4** and have 18-electron configurations. The platinum atom has

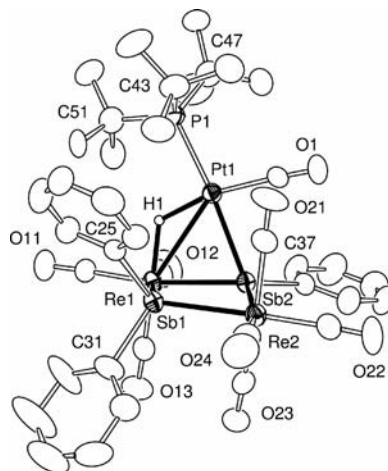


Figure 3. ORTEP diagram of the molecular structure of **4** showing 30% probability thermal ellipsoids. The hydrogen atoms on the ligands are omitted for clarity. Selected interatomic bond distances (Å) are as follows: Pt1–Sb2 2.6493(7), Pt1–Re1 3.0235(5), Re1–Sb2 2.6839(7), Re1–Sb1 2.7744(7), Re2–Sb2 2.7635(7), Re2–Sb1 2.7837(7).

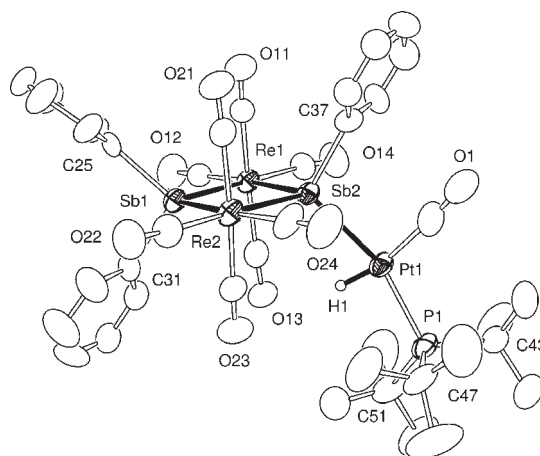


Figure 4. ORTEP diagram of the molecular structure of **5** showing 30% probability thermal ellipsoids. The hydrogen atoms on the ligands are omitted for clarity. Selected interatomic bond distances (Å) are as follows: Pt1–Sb2 2.6100(12), Pt1–H1 1.21(8), Re1–Sb1 2.7572(11), Re1–Sb2 2.8099(12), Re2–Sb1 2.7480(12), Re2–Sb2 2.8015(11).

a 2+ oxidation state and a 16-electron configuration. There is no Re–Re bond present in **4**, Re1···Re2 = 4.413(1) Å.

Compound **5** is similar to **4**, but it contains an additional CO ligand; in fact, it can be made from **4** in 28% by reaction with CO under 1 atm at 25 °C. An ORTEP diagram of the molecular structure of **5** is shown in Figure 4. As with **2–4**, the structure of **5** also contains a Re₂Sb₂ rhombus. Atom Sb2 contains one phenyl ring and a HPt(CO)P(*t*-Bu)₃ group. The Pt–Sb bond distance, Pt1–Sb2 = 2.6100(12) Å, is significantly shorter than the Pt–Sb bond distance in **2**, 2.7166(10) Å. This could be explained by a structural trans influence. Studies have shown that the phosphine ligands generally exhibit a lower structural trans influence than the hydride ligand.¹⁶ This is consistent with the observation that the Pt–Sb bond distance trans to the phosphine ligand in **5** is shorter than the Pt–Sb bond distance in **2**. Similar Pt(H)(CO)(*t*-PBu₃) groups were found coordinated to bridging

(15) Bau, R.; Drabnis, M. H. *Inorg. Chim. Acta* **1997**, 259, 27–50. (b) Teller, R. G.; Bau, R. *Struct. Bonding* **1981**, 41, 1–82.

(16) Kapoor, P.; Kukushkin, V. Y.; Lovgvist, K.; Oskarsson, A. *J. Organomet. Chem.* **1996**, 517, 71–79.

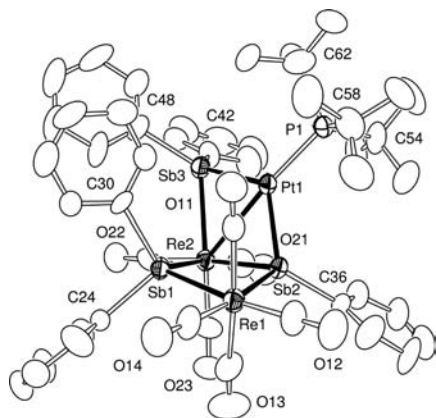
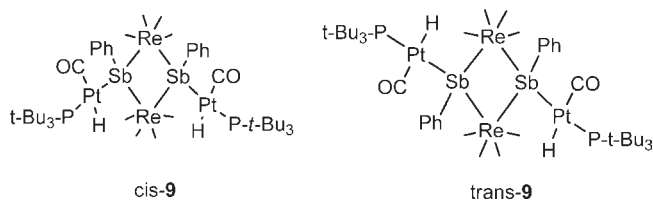


Figure 5. ORTEP diagram of the molecular structure of **6** showing 30% probability thermal ellipsoids. The hydrogen atoms on the ligands are omitted for clarity. Selected interatomic bond distances (Å) are as follows: Pt1–Sb2 2.5166(7), Pt1–Sb3 2.5242(6), Pt1–Re2 2.9297(5), Re1–Sb2 2.7718(7), Re1–Sb1 2.7787(6), Re2–Sb3 2.7461(7), Re2–Sb1 2.7695(6), Re2–Sb2 2.7945(6).

SbPh ligands in the compounds *cis*- and *trans*-**9**.⁵ The phosphine ligands in these compounds also lie *trans* to the Pt–Sb bonds, and they also possess similarly short Pt–Sb bond distances, Pt1–Sb1 = 2.6062(6) Å and Pt2–Sb2 = 2.5957(6) Å in *cis*-**9** and 2.6113(5) Å in *trans*-**9**.



The Re–Sb bond distances to the platinum-substituted antimony atom Sb2, Re1–Sb2 = 2.8099(12) Å and Re2–Sb2 = 2.8015(11) Å, are considerably longer than those to the SbPh₂ group, Re1–Sb1 = 2.7572(11) Å and Re2–Sb1 = 2.7480(12) Å. This is probably due to sterics. The one hydrido ligand H1 (located and refined crystallographically) is terminally coordinated to the platinum atom in a position *trans* to the CO ligand. It exhibits the expected high-field resonance shift in the ¹H NMR spectrum, δ –6.80, with suitable couplings to ³¹P and ¹⁹⁵Pt, ¹J_{Pt–H} = 623 Hz and ²J_{P–H} = 14 Hz. Both rhenium atoms in the 1+ oxidation state in **5** have 18-electron configurations, and the platinum atom (2+ oxidation state) has a 16-electron configuration. There is no Re–Re bond present in **5**, Re1···Re2 = 4.349(1) Å.

The reaction of **4** with SbPh₃ in a solution in *n*-octane solvent at reflux for 2.5 h yielded only one isolable product, **6** (42%). Compound **6** was also characterized crystallographically. An ORTEP diagram of the molecular structure of **6** is shown in Figure 5. Compound **6** is similar to **4** except that it contains one less CO ligand and a bridging SbPh₂ ligand across the Pt–Re bond. The Pt–Sb bond distances are the shortest that we have seen in this series of compounds, Pt1–Sb2 = 2.5166(7) Å and Pt1–Sb3 = 2.5242(6) Å. This may be due to the decreased sterics about the platinum atom as a result of the loss of its terminal CO ligand. The Re–Pt bond distance, Pt1–Re2 = 2.9297(5) Å, is considerably shorter than the corresponding hydride-bridged Re–Pt bond

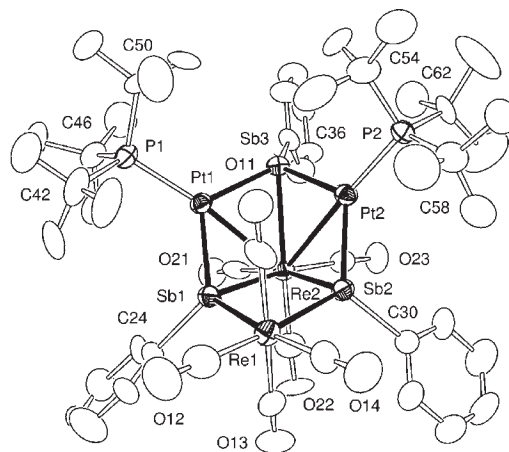
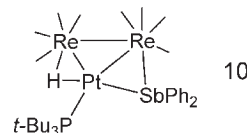


Figure 6. ORTEP diagram of the molecular structure of **7** showing 30% probability thermal ellipsoids. The hydrogen atoms on the ligands are omitted for clarity. Selected interatomic bond distances (Å) are as follows: Pt1–P1 2.259(4), Pt2–P2 2.261(4), Pt1–Sb1 2.5139(11), Pt1–Sb3 2.5323(12), Pt1–Re2 2.9287(9), Pt2–Sb2 2.5161(11), Pt2–Sb3 2.5464(12), Pt2–Re2 2.9139(8), Re1–Sb1 2.7668(12), Re1–Sb2 2.7688(12), Re2–Sb3 2.7526(11), Re2–Sb1 2.7729(12), Re2–Sb2 2.7965(12).

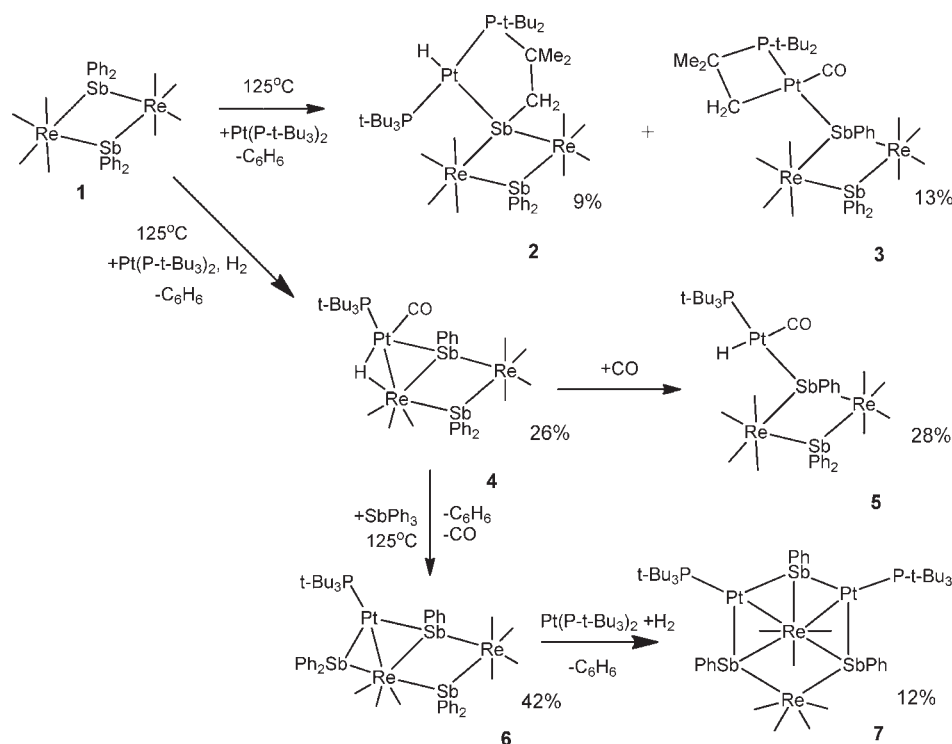
in **4**, 3.0235(5) Å,¹⁵ but it is very similar to the SbPh₂-bridged Pt–Re bond found in the compound Re₂[PtP(*t*-Bu)₃](CO)₈-(μ -SbPh₂)(μ -H) (**10**), 2.9265(3) Å.⁵



Formally, both rhenium atoms have 1+ oxidation states in **6** and 18-electron configurations, and the platinum atom has a 2+ oxidation state and a 16-electron configuration. There is no Re–Re bond present in **6**, Re1···Re2 = 4.413(1) Å. The UV–vis spectrum for **6** in a CH₂Cl₂ solvent exhibits two absorptions: λ_{max} = 418 nm (ϵ = 1.016 × 10⁴ mol^{–1} cm^{–1}) and 485 (3.559 × 10³ mol^{–1} cm^{–1}); see the Supporting Information. Because of the low symmetry and complexity of the molecule, the nature of the electronic transitions responsible for these absorptions cannot be assigned at this time.

The reaction of **6** with Pt[P(*t*-Bu)₃]₂ in a solution in *n*-octane solvent heated to reflux under a purge of hydrogen for 4 h yielded the new compound **7** (12%) as the only isolable metal-containing product. Benzene was detected as a coproduct when the reaction was performed in an NMR tube. An ORTEP diagram of the molecular structure of **7** is shown in Figure 6. Compound **7** contains four metal atoms: two of rhenium and two of platinum. The molecule contains approximate reflection symmetry, but this is not crystallographically imposed. As in each of the compounds **2**–**6**, compound **7** contains a Re₂Sb₂ rhombus. There are three triply bridging SbPh ligands that incorporate two Pt[P(*t*-Bu)₃]₂ groups that bridge ReSb₂ groups. Compounds **4** and **6** each contain one triply bridging SbPh ligand similar to that in **7**, and the series **4** to **6** to **7** represents a controlled cluster growth sequence. The Pt–Sb bond distances, Pt1–Sb1 = 2.5139(11) Å, Pt1–Sb3 = 2.5323(12) Å, Pt2–Sb2 = 2.5161(11) Å, and Pt2–Sb3 = 2.5464(12) Å, are similar to those in **6**, but the Pt–Sb distances to the unique SbPh ligand in **7**, Sb3–Ph, are slightly longer than those to Sb1 and Sb2. The Re–Pt

Scheme 1



distances, $\text{Pt1}-\text{Re2}=2.9287(9)$ Å and $\text{Pt2}-\text{Re2}=2.9139(8)$ Å, are very similar to that in **6**. The $\text{Re}-\text{Sb}$ distances, $\text{Re1}-\text{Sb1}=2.7668(12)$ Å, $\text{Re1}-\text{Sb2}=2.7688(12)$ Å, $\text{Re2}-\text{Sb3}=2.7526(11)$ Å, $\text{Re2}-\text{Sb1}=2.7729(12)$ Å, and $\text{Re2}-\text{Sb2}=2.7965(12)$ Å, are all very similar and similar to those in **4** and **6**. Each platinum atom contains one $\text{P}(t\text{-Bu})_3$ ligand. Atom Re1 contains four linear terminal carbonyl ligands, and atom Re2 has three. Formally, each $\mu_3\text{-SbPh}$ ligand serves as a 4-electron donor, and both rhenium atoms (1+ oxidation state) achieve 18-electron configurations and the two platinum atoms (2+ oxidation state) each have 16-electron configurations. There is no $\text{Re}-\text{Re}$ bond in **7**, $\text{Re1}\cdots\text{Re2}=4.413(1)$ Å. The UV-vis spectrum for **7** exhibits a single low-energy absorption at $\lambda_{\text{max}}=736$ nm ($\epsilon=1.018\times 10^3$ mol $^{-1}$ cm $^{-1}$). Because of the low symmetry and complexity of the molecule, the nature of the electronic transition responsible for this cannot be ascertained at this time. Compounds **6** and **7** were also obtained in low yields, 19% and 10%, respectively, from the reaction of **8** with $\text{Pt}[\text{P}(t\text{-Bu})_3]_2$ when a solution in *n*-octane solvent was heated to reflux for 2 h in the presence of hydrogen gas.

Discussion

In previous studies, it was shown that $\text{Pt}[\text{P}(t\text{-Bu})_3]_2$ reacts with $[\text{Re}(\text{CO})_4(\mu\text{-MPh}_2)]_2$ ($\text{M}=\text{Ge}, \text{Sn}$) by the loss of a $\text{P}(t\text{-Bu})_3$ ligand and the addition of one or two $\text{Pt}[\text{P}(t\text{-Bu})_3]$ groups to the $\text{Re}-\text{Ge}$ and $\text{Re}-\text{Sn}$ bonds of the $[\text{Re}(\text{CO})_4(\mu\text{-MPh}_2)]_2$ compounds (eq 4).¹⁰ By contrast, the reaction of $\text{HRe}(\text{CO})_8(\mu\text{-SbPh}_2)$ ¹¹ with $\text{Pt}[\text{P}(t\text{-Bu})_3]_2$ yielded compound **10** by insertion of the platinum atom into the $\text{Re}-\text{Sb}$ bond (eq 5).⁵

A summary of the reactions reported here is shown in Scheme 1. It has been found that the reaction of **1** with $\text{Pt}[\text{P}(t\text{-Bu})_3]_2$ at 125°C proceeds to the formation of compounds **2** and **3** by a series of steps involving (1) oxidative additions of a $\text{Pt}[\text{P}(t\text{-Bu})_3]$ group to the $\text{Sb}-\text{Ph}$ bond(s) of **1** and a $\text{C}-\text{H}$ bond

of one of the *t*-butyl groups and (2) reductive elimination of the phenyl group and hydrogen atom as benzene. The oxidation state on the platinum atom was increased from zero in the $\text{Pt}[\text{P}(t\text{-Bu})_3]_2$ to 2+ in **3**. Both phenyl groups were cleaved from one of the bridging SbPh_2 ligands in the formation of **2**, and one of the methyl groups on one of the *t*-Bu groups was metalated at the antimony atom to form a five-membered ring containing both that antimony atom and the platinum atom. Details of the sequence of the transformations that ultimately lead to **2** and **3** are not available at this time. Metalation of methyl groups on main group atoms such as antimony is very unusual, but metalation of *t*-Bu groups of $\text{P}(t\text{-Bu})_3$ ligands on platinum is quite common.¹⁴ It seems like **3** could be an intermediate en route to **2**, but our efforts to obtain **2** from **3** have been unsuccessful to date. In further investigations, the reaction of **1** with $\text{Pt}[\text{P}(t\text{-Bu})_3]_2$ was performed under an atmosphere of hydrogen. Under these conditions, neither **2** nor **3** was obtained, but there were two new compounds, **4** and **5**. In the formation of both **4** and **5**, one phenyl group was cleaved from one of the bridging SbPh_2 ligands of **1** and a $\text{Pt}[\text{P}(t\text{-Bu})_3]$ group was added to that antimony atom. Compounds **4** and **5** both contain a CO ligand on the platinum atom and both also contain a hydride ligand, presumably from the supplied hydrogen. In **4**, the platinum atom bridges a $\text{Re}-\text{Sb}$ bond. Compound **5** contains one more CO ligand than **4** and, as expected, **5** can be obtained from **4** by the reaction with CO at 1 atm, but we have not been able to decarbonylate **5** to yield **4**. In the addition of CO to **4**, the bridging platinum atom was shifted to a terminal position on the antimony atom of the SbPh ligand to which it was bonded. Compound **4** also reacts with SbPh_3 in a process that leads to the loss of one CO ligand and the hydride ligand and one phenyl ring from an added molecule of SbPh_3 . The hydride ligand and one phenyl ring are presumably combined to form benzene. The SbPh_2 ligand

that was formed in this reaction occupies a bridging site on the Pt–Re bond that was occupied by the hydride ligand that was present in **4**. In the presence of hydrogen, compound **6** was found to react with an additional quantity of Pt[P(*t*-Bu)₃]₂ to continue the cluster growth process. One phenyl ring was cleaved with the formation of benzene from each of the two SbPh₂ ligands in **6**, a single PtP(*t*-Bu)₃ group was added across these two antimony atoms, and a Pt–Re bond was formed.

In summary, our studies have shown that the PtP(*t*-Bu)₃ group is more aggressive in its reactions at the bridging SbPh₂ ligands in **1** than it is at the bridging SnPh₂ ligands in [Re(CO)₄(μ-SnPh₂)₂]. SbPh ligands are readily formed by cleavage of a phenyl group, and these have been shown to be effective triply bridging ligands that facilitate cluster growth reactions.⁵ We have recently shown that compound **1** is an

effective precursor for supported ReSb nanoparticles that serve as effective catalysts for the ammoxidation of picoline.³ It seems likely that these new ReSbPt complexes might also serve as catalyst precursors for certain types of ammoxidation reactions.

Acknowledgment. This research was supported by the National Science Foundation (Grant CHE-0743190) and the University of South Carolina Nanocenter. We thank Dr. Minglai Fu for assistance in recording of the UV–vis spectra.

Supporting Information Available: CIF files for each of the structural analyses and UV–vis spectra for compounds **6** and **7**. This material is available free of charge via the Internet at <http://pubs.acs.org>.